Tertiary Interactions between the Fifth and Sixth Transmembrane Segments of Rhodopsin†

Mary Struthers, Hongbo Yu, Masahiro Kono, and Daniel D. Oprian*

Department of Biochemistry and Volen Center for Complex Systems, Brandeis University, Waltham, Massachusetts 02454

Received February 2, 1999; Revised Manuscript Received March 23, 1999

ABSTRACT: We have used cysteine scanning mutagenesis and disulfide cross-linking in a split rhodopsin construct to investigate the secondary structure and tertiary contacts of the fifth (TM5) and sixth (TM6) transmembrane segments of rhodopsin. Using a simple increase in pH to promote disulfide bond formation, three cross-links between residues on the extracellular side of TM5 (at positions 198, 200, and 204) and TM6 (at position 276) have been identified and characterized. The helical pattern of cross-linking observed indicates that the fifth transmembrane helix extends through residue 200 but does not include residue 198. Rhodopsin mutants containing these disulfides demonstrate nativelike absorption spectra and light-dependent activation of transducin, suggesting that large movements on the extracellular side of TM5 with respect to TM6 are not required for receptor activation.

Rhodopsin is a prototypic member of the large and diverse family of G protein-coupled receptors (GPCR)[1] which mediate cellular responses to a variety of extracellular ligands and, in the case of rhodopsin, light. The three-dimensional structure of this important class of membrane proteins is of general interest due to the critical roles these receptors play in cellular processes. Due to the inherent difficulty with crystallization of membrane-bound proteins, a precise three-dimensional structure of a GPCR has yet to be obtained. Recent electron cyromicroscopy studies of frog rhodopsin have produced a 7.5 × 16.5 Å electron density map (*1*), while electron cyromicroscopy of bovine rhodopsin has yielded data, some of which is resolved to 3−5 Å (*2*). These studies confirm that the protein consists of seven transmembrane helices arranged in a bundle. Although these maps provide considerable information about the structure of rhodopsin, including relative tilts of the helices, no detailed information on specific tertiary interactions between helices is available.

The lack of precise crystallographic structural information for membrane proteins such as rhodopsin has prompted the development of a number of biochemical methods for investigating the structure of membrane proteins. One such method, which has been used to map out tertiary interactions in the homodimeric bacterial chemotatic receptors, is cysteine scanning mutagenesis and oxidative disulfide cross-linking (*3*−*6*). We have recently adapted this method to monomeric GPCRs such as rhodopsin by utilizing split receptor (SR) constructs in which fully functional receptors are expressed as noncovalently associated N- and C-terminal fragments (*7*). For example, the split receptor constructs we use in the present study contain a break in the cytoplasmic loop between the fifth and sixth transmembrane regions (SR(1−5/6−7)) (Figure 1). To probe tertiary interactions within such a construct, a cysteine is introduced into each fragment and the mutant receptor is subjected to oxidative cross-linking conditions. If a disulfide bond is formed between the introduced cysteines, then these positions are likely to be close in the three-dimensional structure of the native protein. The use of split receptors provides a facile assay for cross-linking between such engineered cysteines; if a disulfide bond is formed, then the protein will migrate on a nonreducing SDS−PAGE gel with an apparent molecular weight similar to that of full-length rhodopsin and significantly greater than that of either fragment. We initially tested this method in rhodopsin by engineering cysteines at positions 204 in the fifth transmembrane region (TM5) and 276 in the sixth transmembrane region (TM6) within SR(1−5/6−7) and demonstrating that a disulfide bond could be formed between these two cysteines (*7*). The choice of these positions was based on the observation that histidine substitutions at analogous positions in a related GPCR, the NK-1 receptor, could form a high-affinity zinc binding site (*8*). On the basis of this work, cysteine scanning and oxidative cross-linking has been used to further investigate the tertiary interactions between the extracellular ends of TM5 and TM6 of rhodopsin.

EXPERIMENTAL PROCEDURES

Materials. 11-*cis*-Retinal was supplied by the National Institutes of Health and Dr. Rosalie Crouch. Dark-adapted bovine retinae were obtained from J. A. Lawson Co. (Lincoln, NE). 1,10-Phenanthroline and *N*-ethylmaleimide (NEM) were from Sigma (St. Louis, MO). [^{35}S]GTPγS (1156

† This work was supported by National Institutes of Health Grant EY07965. M.S. was supported by individual National Research Service Award EY06670. We also acknowledge support for the Volen Center for Complex Systems by the W. M. Keck Foundation.

* To whom correspondence should be addressed.

[1] Abbreviations: NEM, *N*-ethylmaleimide; PBS, 10 mM sodium phosphate, 150 mM NaCl; ConA, concanavalin A; BSA, bovine serum albumin; DTT, dithiothreitol; GPCR, G protein-coupled receptor; buffer B, 2 mM sodium phosphate, 150 mM NaCl, pH 6.0; DM, *n*-dodecyl β-D-maltoside; PMSF, phenylmethanesulfonyl fluoride; TM, transmembrane region; N-terminal, amino-terminal; C-terminal, carboxyl-terminal; ϵ, extinction coefficient.

10.1021/bi9902384 CCC: $18.00
Published on Web 04/24/1999

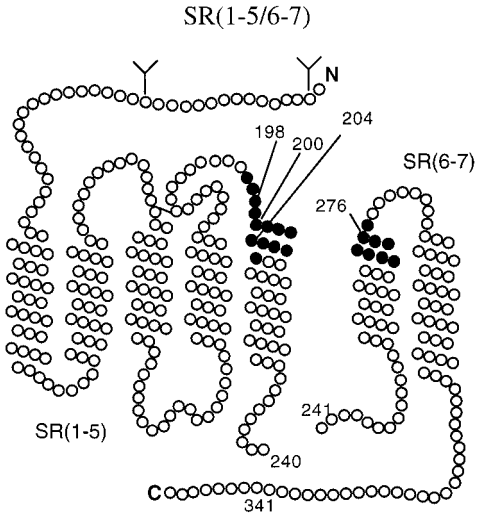

FIGURE 1: Schematic representation of the structure of the split rhodopsin used in this study. The residues mutated to cysteine are shaded. Each fragment is designated by the TM segments encompassed; SR(1−5) refers to the N-terminal fragment consisting of residues 1−240 and transmembrane segments 1−5, and SR(6−7) refers to the C-terminal fragment consisting of residues 241−348 (plus an added initiator methionine) and transmembrane segments 6 and 7.

Ci/mmol) was obtained from NEN, and nonradiolabeled GTPγS was from Boehringer Mannheim. ECL detection reagents and streptavidin-linked horseradish peroxidase for Western blot analysis were obtained from Amersham Life Sciences. The anti-rhodopsin monoclonal antibody 1D4 (*9*, *10*) was purified and coupled to a Sepharose 4B solid support using previously described methods (*11*). Peptide I (Asp Glu Ala Ser Thr Thr Val Ser Lys Thr Glu Thr Ser Gln Val Ala Pro Ala) was purchased from American Peptide Co., Inc. (Santa Clara, CA). V8 protease was obtained from ICN. *n*-Dodecyl β-D-maltoside (DM) was obtained from Calbiochem.

Mutagenesis and Expression of Split Rhodopsin Mutants. The nomenclature for split rhodopsin constructs follows that previously described (*7*): SR(1−5/6−7) refers to a split receptor consisting of an N-terminal fragment containing the first five transmembrane segments (SR(1−5)) and a C-terminal fragment containing the remaining two transmembrane segments (SR(6−7)). The rhodopsin gene fragments were constructed from a synthetic rhodopsin gene in a pMT3-based vector, and cassette mutagenesis was used to create single-residue mutations in the gene fragments as previously described (*7*, *12*). The rhodopsin gene and gene fragments were transiently transfected into COS-1 cells by the DEAE-dextran method using 2 μg of DNA/100-mm plate (*13*). Split receptors were expressed by cotransfection of equal quantities of separate plasmids containing the SR(1−5) gene and the SR(6−7) gene (*7*).

Reconstitution and Purification of Receptors. Transfected COS cells were harvested 72 h posttransfection and either stored at −80 °C or used immediately. Proteins were reconstituted with 11-*cis*-retinal by incubation of harvested cells for 2 h with 11-*cis*-retinal (5 μM) in PBS, pH 6.0 or pH 7.0. Cells were then solubilized in the dark in 1% DM and 1 mM PMSF in PBS and purified by immunoaffinity chromatography using the 1D4-Sepharose 4B matrix in a manner essentially as described previously (*13*). Elution of proteins from 1D4-Sepharose was accomplished with peptide I (0.18 mg/mL) in 0.1% DM in either PBS, pH 7.0, or buffer B (2 mM sodium phosphate, 150 mM NaCl, pH 6.0).

Disulfide Cross-Linking. Disulfide cross-linking of rhodopsin mutants purified in buffer B was promoted by increasing the pH to 8.0 by the addition of 100 mM dibasic sodium phosphate, 150 mM NaCl, followed by incubation for 2 h or overnight (12−18 h) at 25 °C. These reactions were quenched by the addition of gel loading buffer containing NEM (final concentrations 60 mM Tris, pH 6.8, 2% (w/v) SDS, 6% (w/v) sucrose, 0.005% bromophenol blue, and 12.5 mM NEM). Quenched reactions were either analyzed immediately or stored at 4 °C overnight and analyzed by SDS−PAGE and Western blotting the next day.

Absorption Spectroscopy and Western Blot Analysis. UV−visible absorption spectra of immunopurified proteins were acquired on an Hitachi model U-3210 spectrophotometer adapted for dark room use. All spectra were recorded on 1.0-cm path length samples. Data were analyzed using Kalidagraph (Version 3.0.4). Spectra of bleached rhodopsin samples were obtained by illumination with >490-nm light for 1 min followed immediately by data acquisition. Concentrated HCl (to a final concentration of 0.3 M) was added to the bleached rhodopsin samples, the sample was mixed, and data were immediately acquired.

Quenched disulfide cross-linking reactions of immunopurified receptors were subjected to nonreducing 12% polyacrylamide−SDS gel electrophoresis (*14*) followed by transfer to nitrocellulose essentially as previously described (*7*). Concanavalin A was used to detect the carbohydrates on the N-terminal fragment (at positions 2 and 15) of split receptors in Western blot analysis (*15*). After transfer, the nitrocellulose blot was treated with 5% BSA and then incubated with 0.001% (w/v) biotin-ConA in 5% BSA overnight. After washing, the blot was incubated with streptavidin-conjugated horseradish peroxidase, and labeled proteins were visualized with the ECL detection system according to manufacturer directions (Amersham). Purification via the C-terminal 1D4 epitope followed by Western blot detection of the N-terminal fragment ensures that only split receptors consisting of both N- and C-terminal fragments are probed. If a split receptor mutant has been cross-linked, then the protein migrates with a mobility similar to that of full-length, wild-type rhodopsin, while the mobility of a non-cross-linked split receptor is the same as the isolated N-terminal fragment, SR(1−5).

Detection of disulfide bond formation in full-length rhodopsin containing cysteine mutations was accomplished by treatment of the purified proteins in 0.1% DM with V8 protease (0.05 μg/μL) for 2−4 h at room temperature. Reactions were then quenched in SDS loading buffer containing NEM and PMSF (60 mM Tris, pH 6.8, 2% (w/v) SDS, 6% (w/v) sucrose, 0.005% bromophenol blue, 12.5 mM NEM, and 0.7 mM PMSF) and analyzed by the Western blot procedure as described above for the split receptors or by silver staining. Silver staining polyacrylamide gels were performed essentially as in published protocols (*16*). V8 protease cleaves the C-terminal tail of rhodopsin between residues 341 and 342 and in the cytoplasmic loop connecting TM5 and TM6 between residues 239 and 240, producing two major fragments: a C-terminal fragment of ~13 kDa and an N-terminal fragment of >27 kDa, approximately the

same size as SR(1−5) (*17*, *18*). Western blot analysis using ConA as a probe should reveal a protein which migrates with an apparent molecular weight slightly smaller than that of uncut rhodopsin (due to cleavage of the C-terminal seven amino acids) if a cross-link exists between the two fragments.

Transducin Activation. Transducin was purified from bovine retinae as described (*7*) with some modifications (*19*, *20*). The purified protein was dialyzed against 10 mM Tris buffer (pH 7.5) containing 50% (v/v) glycerol and 1 mM $MgCl_2$. The ability of purified split receptors to catalyze the exchange of GDP for radiolabeled [^{35}S]GTPγS in transducin was examined using a filter binding assay as has been described (*7*, *21*). Purified receptors were used in these assays at concentrations of either 15 or 5 nM in 0.01% DM. The concentration of mutant and wild-type receptors was determined by absorption spectroscopy from the absorbance at 500 nm ($\epsilon = 40\,600$) (*21*), based on the assumption that the extinction coefficient for the mutants does not differ from that of wild-type rhodopsin.

RESULTS

Cross-Linking of Cysteine Substitutions in TM5 with F276C in TM6. Single cysteine substitutions from positions 196 to 208 on the extracellular side of TM5 were constructed in SR(1−5) and coexpressed with a C-terminal fragment SR(6−7) containing a F276C mutation. Split receptors were initially purified at pH 6.0 in buffer B, the pH subsequently was raised to 8.0 by addition of dibasic phosphate, and the sample was incubated for 2 h at 25 °C to induce disulfide bond formation. The reactions were then analyzed by SDS−PAGE and Western blot (Figure 2). Split receptors containing cysteine substitutions at positions 203 and 206 were expressed at very low levels in COS cells. Mutations of these positions in the full-length receptor have previously been noted to result in low expression levels (A. Kumbasar and D. D. Oprian, unpublished results). Although not visible due to low expression levels in the Western blot of the experiment shown in Figure 2B, analysis of a more concentrated sample of SR(1−5:F203C/6−7:F276C) in a separate experiment indicated that it is not significantly cross-linked under these conditions (Figure 2C).

Cysteine substitutions at positions 198, 200, and 204 in SR(1−5) exhibited significant cross-linking with cysteine at position 276 in SR(6−7) using this mild oxidation strategy, although these cysteines differed in their reactivity for disulfide bond formation, as illustrated in Figure 2. SR(1−5:N200C/6−7:F276C) is spontaneously cross-linked in the purified protein at pH 6.0. SR(1−5:V204C/6−7:F276C) can be isolated predominately in the reduced form at pH 6.0, while incubation at pH 6.0 for 2 h leads to partial cross-linking, and incubation at pH 8 will readily cross-link these fragments in less than 2 h. In comparison, cysteine at position 198 is less reactive to cross-linking with position 276 and complete cross-linking requires treatment at pH 8 for more than 2 h.

Mutant split receptors containing single cysteine substitutions at 198, 200, or 204 in SR(1−5) paired with wild-type SR(6−7) or wild-type SR(1−5) paired with SR(6−7:F276C) were not cross-linked under any of these conditions tested, indicating that the cross-linking observed in the double mutants illustrated in Figure 2 required mutations of both

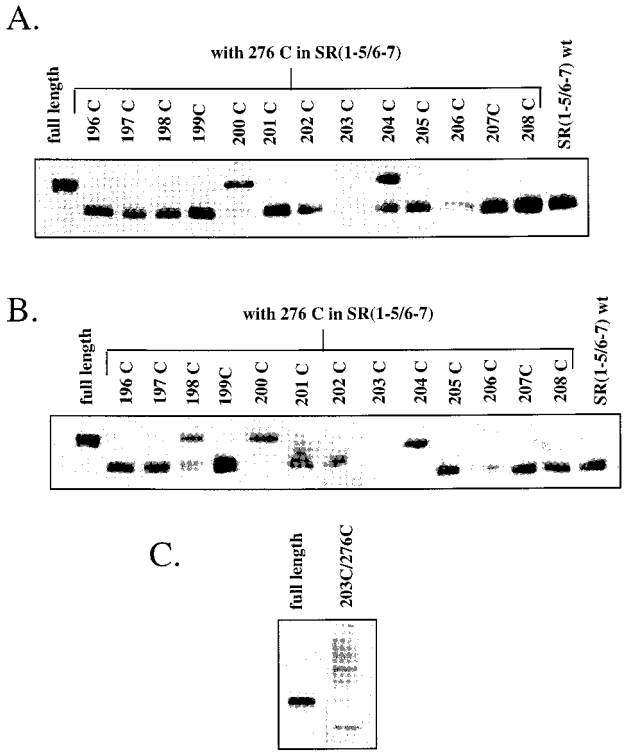

FIGURE 2: Disulfide cross-linking reactions between single cysteine substitutions at positions 196−208 and Cys276 in SR(1−5/6−7). A. ConA blot analysis of mutant split receptors treated at pH 6.0 and 25 °C for 2 h immediately following purification. B. ConA blot analysis of cross-linking at pH 8.0 and 25 °C for 2 h immediately following purification at pH 6.0. Equal protein amounts were loaded for SDS−PAGE analysis based on absorbance of the pigments, with the exception of SR(1−5:203C/6−7:276C) and SR(1−5:206C/6−7:276C) which were obtained in insufficient quantities to record absorption spectra and therefore the maximum sample volume was loaded. C. SDS−PAGE and ConA blot analysis of SR(1−5:203C/6−7:276C) incubated at pH 8.0 for 2 h at 25 °C.

positions to cysteine and is therefore specifically attributable to disulfide bond formation between the introduced cysteines. Additionally, cysteine scanning of TM6 between residues 270 and 277 in SR(6−7), paired with single cysteine substitution at position 198, 200, 204 or 208, did not reveal any additional cross-links (data not shown). Thus, the only cysteine substitution in the region of TM6 that cross-links with TM5 under these mild conditions is 276.

Absorbance Spectra of Cysteine Mutants. Both SR(1−5:T198C/6−7:F276C) and SR(1−5:V204C/6−7:F276C) receptors can be reconstituted with 11-*cis*-retinal to form functional pigments exhibiting a 500-nm absorbance maximum characteristic of the correctly folded dark-state rhodopsin. This signature absorbance maximum is maintained after oxidation of the cysteines to the disulfide (Figures 3A and 4A). The cross-linked receptors also exhibited normal bleaching behavior: illumination at >490-nm light produced a 380-nm maximum absorbance indicative of the deprotonated Schiff base form of the covalently bound *all-trans*-retinal in metarhodopsin II. This was further confirmed by addition of HCl which denatures the protein and traps the Schiff base in the protonated form with an absorbance maximum at 440 nm (Figures 3A and 4A).

Reconstitution of SR(1−5:N200C/6−7:F276C) with 11-*cis*-retinal yielded very low or undetectable pigment levels

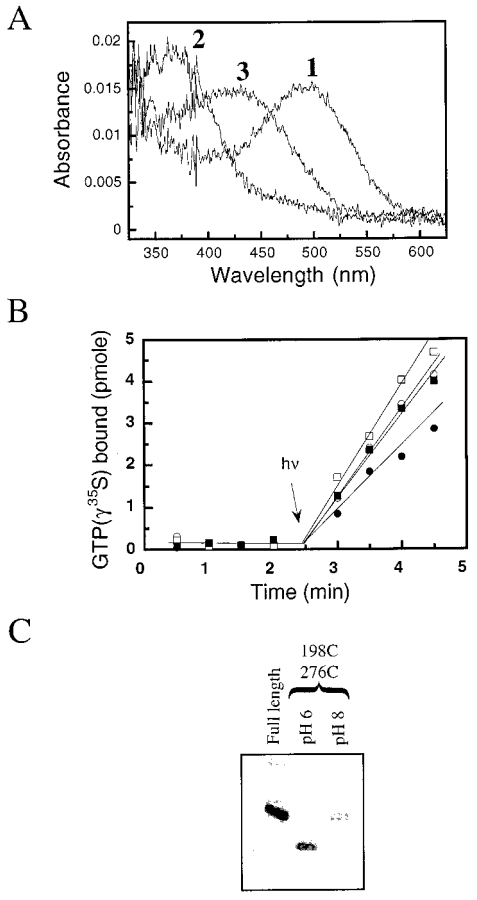

FIGURE 3: Functional analysis of SR(1−5:T198C/6−7:F276C). A. Spectral properties of the cross-linked form of SR(1−5:T198C/6−7:F276C) obtained by overnight incubation at pH 8.0: 1, dark-state spectrum; 2, after illumination of 1 with >490-nm light for 2 min; 3, acidification of 2 with HCl. B. Transducin activation by SR(1−5:T198C/6−7:F276C) and the wild-type split receptor, SR(1−5/6−7): ■, un-cross-linked SR(1−5:T198C/6−7:F276C) after purification at pH 6.0; ●, SR(1−5:T198C/6−7:F276C) cross-linked by overnight incubation at pH 8.0, 25 °C; □, SR(1−5/6−7) after purification at pH 6.0; ○, SR(1−5/6−7) after overnight incubation at pH 8.0. Concentration of all receptors was 15 nM as determined by absorbance at 500 nm. C. Western analysis showing the reduced and cross-linked forms of SR(1−5:T198C/6−7:276C) analyzed in B.

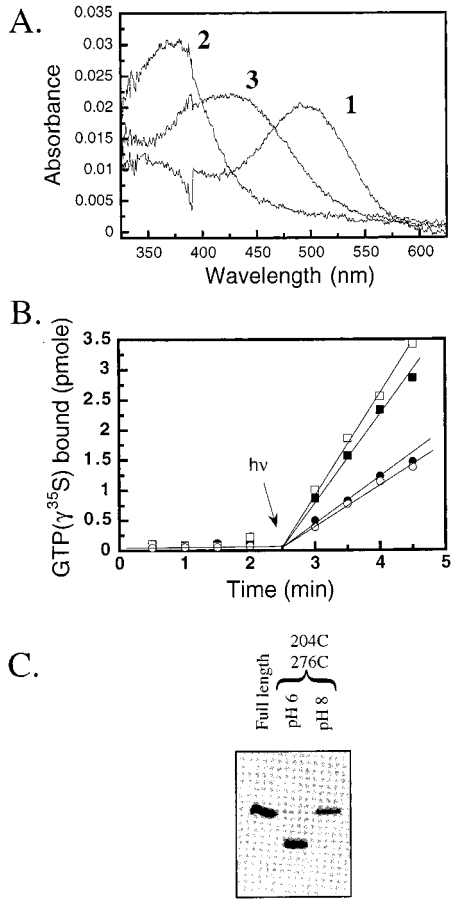

FIGURE 4: Functional analysis of SR(1−5:V204C/6−7:F276C). A. Spectral properties of the cross-linked form of SR(1−5:V204C/6−7:F276C) obtained by overnight incubation at pH 8.0: 1, dark-state spectrum; 2, illumination of 1 with >490-nm light for 2 min; 3, acidification of 2 with HCl. B. Transducin activation by SR(1−5:V204C/6−7:F276C) and the wild-type split receptor, SR(1−5/6−7): ■, reduced SR(1−5:V204C/6−7:F276C) after treatment with 0.7 mM DTT at pH 6.0 for 2 h at 25 °C; ●, cross-linked SR(1−5:V204C/6−7:F276C) after 2 h at 25 °C and pH 8.0; □, SR(1−5/6−7) after treatment with 0.7 mM DTT at pH 6.0 for 2 h at 25 °C; ○, SR(1−5/6−7) after 2 h at 25 °C at pH 8.0. Concentration of all receptors was 5 nM as determined by the absorbance at 500 nm. C. Western analysis showing the reduced and cross-linked forms of SR(1−5:V204C/6−7:F276C) analyzed in B.

as indicated by low absorbance values at 500 nm obtained from purified samples. Western analysis revealed that this double mutant was purified in the cross-linked form at pH 6.0 (Figure 2A) but was expressed at lower levels than the other split receptor mutants (data not shown). Also contributing to the poor reconstitution of SR(1−5:N200C/6−7:F276C) may be a potentially reduced stability toward thermal chromophore loss as has been observed for the cross-linked form of SR(1−5:V204C/6−7:F276C); although stable at 25 °C, treatment of SR(1−5:V204C/6−7:F276C) at 37 °C leads to rapid chromophore loss (data not shown). Consequently, spectroscopic detection of a pigment was difficult for the 200C/276C double mutant in the split receptor, and the effect of the 200−276 cross-link on retinal binding and activity could not be adequately assessed.

The levels of expression and reconstitution of the wild-type split receptor SR(1−5/6−7) are approximately 30−50% of that obtained for full-length rhodopsin (*7*). The N200C,-F276C double mutant was therefore constructed in full-length opsin (designated FL 200C,276C) in the hope that it would be expressed at higher levels and have increased stability, thus allowing for the unambiguous assessment of the effect of the 200−276 cross-link on pigment formation and activity. Western blot analysis and silver staining of purified samples of FL 200C,276C indicate that expression of this mutant was typically 25−50% of that observed for wild-type, full-length rhodopsin (FL-wt) or the full-length, single mutants (FL 200C or FL 276C; data not shown), consistent with the relatively low levels of expression observed for the double mutant in the split receptor.

Digestion with V8 protease which cleaves rhodopsin between TM5 and TM6 was used to investigate the oxidation state of the Cys200−Cys276 pair in FL 200C,276C. Digestion of FL-wt with V8 protease followed by Western blot analysis with ConA reveals the expected N-terminal fragment of approximately 27 kDa (Figure 5). In contrast, digestion of FL 200C,276C with V8 protease produces an N-terminal fragment that migrates on SDS−PAGE gels only slightly faster than the uncut sample, as would be expected if a disulfide existed between the cleaved N- and C-terminal

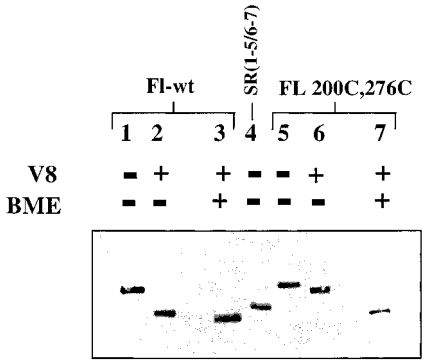

FIGURE 5: V8 digestion and Western analysis of FL 200C,276C illustrating the presence of the 200−276 disulfide. The N-terminus of rhodopsin was detected in purified samples using ConA. The same amount of FL 200C,276C and FL-wt as determined by absorption spectroscopy was used for Western analysis. SR(1−5/6−7) is included as a molecular weight marker. Lanes 1−3, FL-wt: V8 digestion produces an N-terminal fragment significantly smaller than observed for the uncut sample, compare lanes 1 and 2. Lanes 5−7 FL 200C,276C: V8 digestion produces an N-terminal fragment which runs with an apparent molecular weight only slightly smaller than that observed for uncut FL 200C,276C, compare lanes 5 and 6. Addition of BME to the V8 digest of FL 200C,276C (lane 7) reduces this disulfide, and the sample runs with the same apparent MW as similarly treated FL-wt (compare lanes 3 and 7).

fragments. Addition of BME to load buffer prior to SDS−PAGE analysis of the V8 digestion of FL-wt results in only a small shift in the mobility of the N-terminal fragment presumably due to the reduction of the native 110−187 disulfide (lanes 2 and 3, Figure 5). In contrast, BME treatment of the V8 digests of FL 200C,276C produced an N-terminal fragment signficantly smaller than that obtained under nonreducing conditions and of the same size as that obtained by the BME treatment of FL-wt (lanes 3 and 7, Figure 5). This demonstrates that a disulfide exists between Cys200 and Cys276 in FL 200C,276C after purification. Spectral analysis of cross-linked FL 200C,276C reconstituted with 11-*cis*-retinal revealed a peak with an absorbance maximum at 500 nm characteristic of a correctly folded rhodopsin (Figure 6A). Pigment (A_{500}) levels were approximately 25−50% of that obtained for wild-type rhodopsin consistent with the SDS−PAGE analysis, indicating that the majority of purified protein correctly bound 11-*cis*-retinal. Therefore, formation of the 200−276 disulfide in FL 200C,276C does not affect 11-*cis*-retinal binding, nor does it significantly alter the dark-state structure.

Transducin Activation by Cross-Linked Rhodopsins. The mutant split receptors which exhibited significant cross-linking were further analyzed for their ability to activate the G protein transducin in a light-dependent manner. The reduced forms of SR(1−5:V204C/6−7:F276C) and SR(1−5:T198C/6−7:F276C) activated transducin in a light-dependent manner (Figures 3B and 4B). Significantly, the disulfide cross-linked forms of both SR(1−5:V204C/6−7:F276C) and SR(1−5:T198C/6−7:F276C) also activated transducin in a light-dependent manner indistinguishable from the wild-type split receptor SR(1−5/6−7) (Figures 3B and 4B). The oxidation state of the split receptors was confirmed by Western analysis (Figures 3C and 4C). The addition of DTT (0.7 mM) to purified samples of SR(1−5:V204C/6−7:F276C) was required to maintain the completely

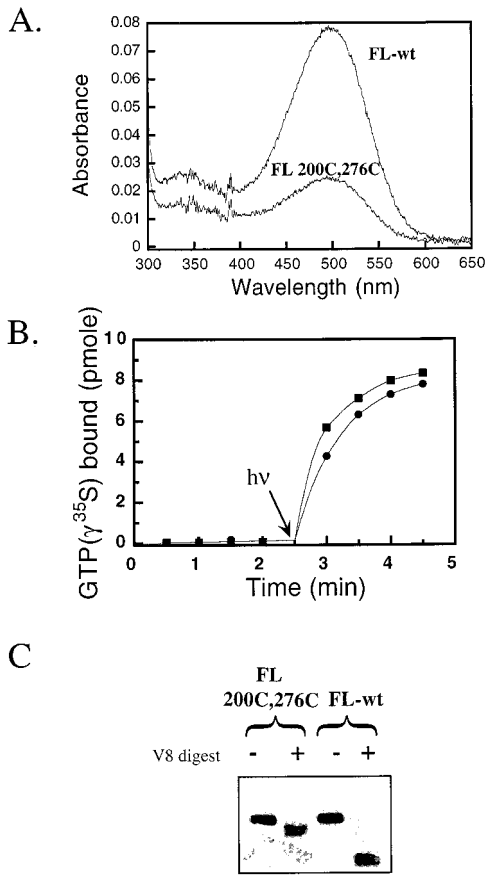

FIGURE 6: Functional analysis of FL 200C,276C. A. Spectra of FL 200C,276C and FL-wt. B. Activation of transducin by FL 200,-276C (●) and FL-wt (■). Each assay contained 5 nM pigment as determined by the absorbance at 500 nm. C. V8 protease digestion and ConA Western analysis of FL 200,276C and FL-wt.

reduced state of the purified receptor during analysis; DTT had a slight activating effect on the reactivities of both the wild-type and mutant receptors as has been observed previously (H. Yu and D. D. Oprian, unpublished results). The cross-linked form of FL 200C,276C also activated transducin similarly to FL-wt (Figure 6B). The presence of the 200−276 disulfide in of FL 200C,276C was confirmed by V8 digestion and Western analysis (Figure 6C). Thus, all three cross-links are compatible with the structural rearrangements required for activation of rhodopsin.

DISCUSSION

We and others have previously reported the development of a method for mapping tertiary contacts within monomeric membrane proteins using cysteine scanning mutagenesis and oxidative cross-linking within split protein constructs (*7*, *22*). On the basis of work with the bacterial chemotatic receptors (*3*), disulfide bond formation was catalyzed by addition of copper phenanthroline ($Cu(phen)_3^{2+}$) (*23*). Cysteine substitutions at positions 204 and 276 in TM5 and TM6 of rhodopsin were used to test this method on rhodopsin. Cysteine mutations at 204 and 276 in split rhodopsin SR(1−5/6−7) were cross-linked upon treatment with the oxidant $Cu(phen)_3^{2+}$ (*7*). Our initial attempts to expand on these results and use cysteine scanning and oxidative cross-linking to further investigate this region of the receptor employed $Cu(phen)_3^{2+}$ as the cross-linking agent (*24*). Although a limited

set of residues was observed to rapidly and completely cross-link upon treatment with $Cu(phen)_3^{2+}$, extensive partial (<10%) cross-linking was also observed for many residues in both helices (data not shown), indicating that oxidation by this reagent is not sufficiently selective and is perhaps trapping local dynamic movements. A milder oxidation strategy was therefore desired and a procedure using a simple increase in pH to promote disulfide bond formation was used. Cross-linking induced by an increase in pH produces a pattern of cross-linking which is similar to the pattern of rapid and complete cross-links observed using $Cu(phen)_3^{2+}$ without the ubiquitous partial cross-linking observed for that method.

Using this method, cysteine scanning and oxidative cross-linking was used to further investigate tertiary contacts in the TM5 and TM6 regions of the intradiscal side of rhodopsin (Figure 1). A series of single cysteine mutations from residues 196 to 208 in TM5 of SR(1−5) was coexpressed with SR(6−7:F276C) and tested in the cross-linking assay. Three cross-links were identified and characterized from these efforts; positions 198, 200, and 204 in TM5 were found to selectively cross-link to position 276 in TM6 (Figure 2). The use of this mild oxidation strategy places a stringent requirement on the proximity of these residues in the tertiary structure of rhodopsin. The α carbons of disulfide-bonded cysteines in proteins are less than 7 Å from each other (*25*, *26*). The rate of disulfide bond formation has been used to indicate the relative distance between the reactive cysteines in previous structural studies using cysteine scanning and oxidative cross-linking methods (*4*, *27*). Although there may be other factors such as disulfide bond geometry and access to oxidant which influence the rate of disulfide bond formation, the collision rate between the two thiols which is related to the interresidue distance is likely to play a principal role. The differing reactivities of these cysteines at positions 198, 200, and 204 for disulfide bond formation with cysteine at 276 suggest that the distances between these residues and position 276 vary; position 200 appears to be closest to position 276 followed by position 204 and more distally position 198. The spontaneous cross-linking observed for SR(1−5:N200C/6−7:F276C) indicates that disulfide bond formation may occur in the opsin state while the protein is still in the intact cell or during solubilization and purification of the split receptor.

All split receptor constructs were tested for the ability to generate a pigment upon reconstitution with 11-*cis*-retinal. Generation of the characteristic absorbance maximum at 500 nm is an indication of a correctly folded dark-state structure of the receptor. Although attempts to reconstitute SR(1−5:N200C/6−7:F276C) with 11-*cis*-retinal produced either very small or undetectable levels of pigment (A_{500}), the double mutant in full-length rhodopsin (FL 200C,276C) produced a protein with a wild-type-like spectrum. Thus, although the 200,276 double cysteine mutation may have some effect on stability and expression levels, the 200−276 disulfide does not appear to interfere with 11-*cis*-retinal binding or pigment formation. Split receptors SR(1−5:V204C/6−7:F276C) and SR(1−5:198C/6−7:F276C) also generated wild-type-like pigments (A_{500}) in both the reduced and cross-linked forms, indicating that all three of these cross-links are compatible with the native dark-state rhodopsin structure.

The pattern of cross-linking observed in rhodopsin agrees with previous studies of the GPCR NK-1 receptor in which histidine residues placed at 193, 197, and 272 (corresponding to 200, 204, and 276 in rhodopsin numbering) formed a high-affinity zinc binding site as measured by disruption of agonist binding (*8*). Sequence comparison (*28*), hydrophobicity, and modeling studies (*29*, *30*) of GPCRs have predicted that these positions (200, 204, and 276) belong to transmembrane helices 5 and 6, although a recent model has placed residue 200 in the loop region between TM4 and TM5 (*31*). The selective disulfide cross-linking of rhodopsin observed in this study is consistent with a helical conformation for residues 200−208 of the receptor, which would place 200 and 204 on the same face of the helix. Importantly, cysteine substitution at position 276 was observed to cross-link only to residues 200 and 204 and no other positions from 200 to 208. In contrast, the disulfide cross-linking of positions 198 and 276 in rhodopsin is not compatible with the transmembrane helix extending into this region of the protein sequence; a continuous helical structure would place positions 198 and 200 on opposite faces of the helix. Consistent with this observation, modeling studies have placed residue 198 in the loop region between TM4 and TM5 (*28*, *31*). The observation that disulfides between all three cysteine pairs do not impair 11-*cis*-retinal binding and pigment formation indicates that the helical structure suggested by these results is present in the native dark-state rhodopsin structure.

In addition to normal pigment formation, mutant rhodopsins containing a disulfide at 198−276, 204−276, or 200−276 are capable of activating transducin in a light-dependent manner with specific activity comparable to that of wild-type controls. Thus, all three disulfides are compatible with the structural rearrangement which occurs upon light activation of the receptor. Only small changes in the distance between residues 198, 200, or 204 and 276 would be possible in the disulfide cross-linked proteins implying that the relative position of the extracellular end of TM5 and position 276 in TM6 is similar in both the light-activated and dark-state of rhodopsin assuming no structural deformation results from the cross-links. The validity of this assumption is supported by both the helical pattern of cross-linking observed and the wild-type spectral properties of the cross-linked receptors studied. Recent studies of the cytoplasmic surface of rhodopsin employing disulfide cross-links (*18*), spin labeling (*18*), and engineered metal binding sites (*32*) have suggested that significant movement of the cytoplasmic end of TM6 is a requirement for receptor activation. Our results indicate that large movements of TM5 relative to TM6 in the extracellular region of rhodopsin are unlikely to be a requirement for receptor activation.

Although significant progress has been made toward the structural elucidation of the GPCR rhodopsin, the difficulty in membrane protein crystallization has made the generation of a high-resolution structure an elusive goal. Recent electron density maps from cyromicroscopy studies combined with modeling work has provided a glimpse at the helical bundle structure of the receptor. Models of the structure of rhodopsin based on the cyromicroscopy maps and sequence homology analysis must rely on other data for confirming important structural constraints, such as the register of the protein sequence within the rods of electron density seen in the map. Biochemical studies employing a variety of techniques

including site-directed spin labeling (*33*, *34*) and the engineering of metal binding sites (*8*, *32*, *35*, *36*) and disulfides (*7*, *18*, *37*) have helped to provide such information. The cysteine scanning and cross-linking study described here adds to this base of knowledge by demonstrating the proximity of TM5 and TM6 on the extracellular side of rhodopsin and suggesting the limits of helical structure within the extracellular end of TM5. In addition, the analysis of the functional consequences of cross-linking in this region of the receptor suggests the structural rearrangement which occurs upon receptor activation does not involve the relative movement of the extracellular ends of TM5 and TM6.

ACKNOWLEDGMENT

Jeffry Fasick is gratefully acknowledged for critical reading of this manuscript.

REFERENCES

1. Unger, V. M., Hargrave, P. A., Baldwin, J. M., and Schertler, G. R. X. (1997) *Nature 389*, 203−206.
2. Krebs, A., Villa, C., Edwards, P. C., and Schertler, G. F. X. (1998) *J. Mol. Biol. 282*, 991−1003.
3. Falke, J. J., and Koshland, D. E., Jr. (1987) *Science 237*, 1596−1600.
4. Lee, G. F., Burrows, G. G., Lebert, M. R., Dutton, D. P., and Hazelbauer, G. L. (1994) *J. Biol. Chem. 269*, 29920−29927.
5. Pakula, A. A., and Simon, M. I. (1992) *Proc. Natl. Acad. Sci. U.S.A. 89*, 4144−4148.
6. Chervitz, S. A., Lin, C. M., and Falke, J. J. (1995) *Biochemistry 34*, 9722−9733.
7. Yu, H., Kono, M., McKee, T. D., and Oprian, D. D. (1995) *Biochemistry 34*, 14963−14969.
8. Elling, C. E., Møller Nielsen, S., and Swartz, T. W. (1995) *Nature 374*, 74−77.
9. Molday, R. S., and MacKenzie, D. (1983) *Biochemistry 22*, 653−660.
10. MacKenzie, D., Arendt, A., Hargrave, P., McDowell, J. H., and Molday, R. S. (1984) *Biochemistry 23*, 6544−6459.
11. Cuatrecasas, P. (1970) *J. Biol. Chem. 245*, 3059−3065.
12. Ferretti, L., Karnik, S. S., Khorana, H. G., Nassal, M., and Oprian, D. D. (1986) *Proc. Natl. Acad. Sci. U.S.A. 83*, 599−603.
13. Oprian, D. D. (1993) *Methods Neurosci. 15*, 301−306.
14. Laemmli, U. K. (1970) *Nature 227*, 680−685.
15. Kono, M., Yu, H., and Oprian, D. D. (1998) *Biochemistry 37*, 1302−1305.
16. Merril, C. R., Goldman, D., Sedman, S. A., and Ebert, M. H. (1981) *Science 211*, 1437−1438.
17. Pappin, D. J., and Findlay, J. B. (1984) *Biochem. J. 217*, 605−613.
18. Farrens, D. L., Altenbach, C., Yang, K., Hubbell, W. L., and Korana, H. G. (1996) *Science 274*, 768−770.
19. Wessling-Resnick, M., and Johnson, G. L. (1987) *J. Biol. Chem. 262*, 3697−3705.
20. Baehr, W., Morita, E. A., Swanson, R. J., and Applebury, M. L. (1982) *J. Biol. Chem. 257*, 6452−6460.
21. Zhukovsky, E. A., Robinson, P. R., and Oprian, D. D. (1991) *Science 251*, 558−560.
22. Wu, J., and Kaback, H. R. (1996) *Proc. Natl. Acad. Sci. U.S.A. 93*, 14498−14502.
23. Kobashi, K. (1968) *Biochim. Biophys. Acta 158*, 239−245.
24. Kono, M., Yu, H., and Oprian, D. D. (1996) *Biophys. J. 70*, W-Pos94.
25. Katz, B. A., and Kossiakoff, A. (1986) *J. Biol. Chem. 261*, 15480−15485.
26. Richardson, J. S. (1981) *Adv. Protein Chem. 34*, 167−339.
27. Stoddard, B. L., Bui, J. D., and Koshland, D. E., Jr. (1992) *Biochemistry 31*, 11978−11983.
28. Donnelly, D., Findlay, J. B. C., and Blundell, T. L. (1994) *Receptors Channels 2*, 61−78.
29. Donnelly, D., and Findlay, J. B. C. (1994) *Curr. Opin. Struct. Biol. 4*, 582−589.
30. Baldwin, J. M. (1993) *EMBO J. 12*, 1693−1703.
31. Baldwin, J. M., Schertler, G. F., and Unger, V. M. (1997) *Mol. Biol. 272*, 144−164.
32. Sheikh, S. P., Zvyaga, T. A., Lichtarge, O., Sakmar, T. P., and Bourne, H. R. (1996) *Nature 383*, 347−350.
33. Farahbakhsh, Z. T., Ridge, K. D., Khorana, H. G., and Hubbell, W. L. (1995) *Biochemistry 34*, 8812−8819.
34. Altenbach, C., Yang, K., Farrens, D. L., Farabakhsh, Z. T., Khorana, H. G., and Hubbell, W. L. (1996) *Biochemistry 35*, 12470−12478.
35. Elling, C. E., and Schwartz, T. W. (1996) *EMBO J. 15*, 6213−6219.
36. Thirstrup, K., Elling, C. E., Hjorth, S. A., and Schwartz, T. W. (1996) *J. Biol. Chem. 271*, 7875−7878.
37. Yang, K., Farrens, D. L., Altenbach, C., Farahbakhsh, Z. T., Hubbell, W. L., and Khorana, H. G. (1996) *Biochemistry 35*, 14040−14046.

BI9902384